REGRESSION RELATIONSHIPS BETWEEN SATELLITE INFRARED RADIANCES AND GEOPOTENTIAL HEIGHTS OF THE 500 MB AND 300 MB LEVELS

Robert Alan Stanfield

NAVAL POSTGRADUATE SCHOOL
Monterey, California

THESIS

REGRESSION RELATIONSHIPS BETWEEN SATELLITE INFRARED RADIANCES AND GEOPOTENTIAL HEIGHTS OF THE 500 MB AND 300 MB LEVELS

by

Robert Alan Stanfield

Thesis Advisor: F. L. Martin

March 1972

Approved for public release; distribution unlimited.

Regression Relationships between Satellite Infrared Radiances and Geopotential Heights of the 500 mb and 300 mb Levels

by

Robert Alan Stanfield
Lieutenant, United States Navy
B.S., United States Naval Academy, 1965

Submitted in partial fulfillment of the
requirements for the degree of

MASTER OF SCIENCE IN METEOROLOGY

from the

NAVAL POSTGRADUATE SCHOOL
March 1972

ABSTRACT

Least squares methods are used with NIMBUS IV SIRS-B clear-column radiances as independent variables and two identical-period sources of geopotential heights (at the 500 mb and 300 mb pressure levels) as dependent variables. Regression equations are developed for each of the sets of geopotential heights for three latitude bands in the Northern Hemisphere. Three-day and four-day data bases were used on each regression specification. Each set of equations was tested on independent data at a subsequent composite period of 12-hours and 24-hours following the dependent pooled samples. The regression results of both the dependent and independent tests were examined for possible operational usefulness.

TABLE OF CONTENTS

I. INTRODUCTION ---------- 12

II. DATA PROCESSING ---------- 19

  A. THE ORIGINAL NESC DATA ---------- 19

  B. FNWC DATA ---------- 24

III. DEPENDENT DATA REGRESSIONS ---------- 25

  A. DEVELOPMENT OF REGRESSION EQUATIONS USING NESC GENERATED VALUES OF 500 MB AND 300 MB GEOPOTENTIAL HEIGHTS ---------- 25

  B. DEVELOPMENT OF REGRESSION EQUATIONS USING FNWC-INTERPOLATED VALUES OF 500 MB AND 300 MB GEOPOTENTIAL HEIGHTS ---- 31

  C. COMPARISONS BETWEEN NESC AND FNWC DEPENDENT REGRESSION ANALYSES ---------- 36

IV. INDEPENDENT SAMPLE TESTS ---------- 40

  A. VERIFICATION PROCEDURE FOR THE INDEPENDENT DATA TESTS ---------- 40

  B. SUMMARY OF INDEPENDENT TEST RESULTS ---------- 46

    1. Results Internal to the Independent Data Tests ---------- 46

    2. Comparison of Independent- With Dependent- Data Specification ---- 48

V. CONCLUSIONS ---------- 51

APPENDIX - COMPUTER PROGRAM FOR GRIDDING AND INTERPOLATION ---------- 53

LIST OF REFERENCES ------------------------------------ 57

INITIAL DISTRIBUTION LIST ----------------------------- 58

FORM DD 1473 -- 59

LIST OF TABLES

1. Height and Temperature Regression Coefficients for September 1969 ---------------------------------- 16
2. 500 mb NESC Dependent Regression Coefficients for Three- and Four-day Data Base, Giving Best Fit for Equation (8) ---------------------------- 27
3. 300 mb NESC Dependent Regression Coefficients for Three- and Four-day Data Base, Giving Best Fit for Equation (8) ---------------------------- 28
4. R^2 and Standard Errors (gpm) for NESC Dependent Regression Equations for 500 mb and 300 mb Three- and Four-day Samples --------------------- 30
5. 500 mb FNWC Dependent Regression Coefficients for Three- and Four-day Data Base ------------------ 32
6. 300 mb FNWC Dependent Regression Coefficients for Three- and Four-day Data Base --------------- 33
7. R^2 and Standard Errors (gpm) for FNWC Dependent Regression Equations for 500 mb and 300 mb Three- and Four-day Dependent Samples ----------- 35
8. Summary of NESC and FNWC Dependent Regression Test Results ------------------------------------ 37
9. Verification Resulting from the Use of Equation (8) upon 500 mb NESC Independent Data -- 42
10. Verification Resulting from the Use of Equation (8) upon 300 mb NESC Independent Data ----------- 43

11. Verification Resulting from the Use of Equation (8) upon 500 mb FNWC Independent Data ---------------- 44

12. Verification Resulting From the Use of Equation (8) upon 300 mb FNWC Independent Data ---------------- 45

13. Summary of NESC and FNWC Independent Regression Test Results Using Equation (8) ------------------ 47

14. Summary of Dependent to Independent Test Shrinkage-- 50

LIST OF FIGURES

1. Derivative of transmittance with respect to the logarithm of pressure for eight SIRS-A channels [after Smith et al (1970)] .

TABLE OF SYMBOLS AND ABBREVIATIONS

A	Fractional amount of estimated cloud cover
$B[\nu, T]$	Planck radiance at wave number ν and temperature T
C_o	Regression equation constant
C_i	Regression equation coefficient for channel i
CO_2	Carbon dioxide
cm	centimeter
D_o	Regression equation constant
D_1	Regression equation coefficient
F_o	Regression equation constant
F_1	Regression equation coefficient
FNWC	Fleet Numerical Weather Central
GMT	Greenwich Mean Time
i	Channel number index
j	Pressure level index
k	Number of predictors

K	Kelvin temperature (degrees)
lnp	Natural logarithm of pressure
m	Meter
mb	Millibar
n	Sample size
N	Observed radiance
N_c	Cloud corrected radiance
N_i	Observed radiance for channel i
NASA	National Aeronautics and Space Administration
NESC	National Environmental Satellite Center
p	pressure or pressure level
p_s	pressure at surface
R	correlation coefficient
R^2	Explained fraction variance
$1-R^2$	Unexplained fractional variance
std. dev.	Standard deviation
std. error	Standard error
T	Temperature, °K

T_B	Brightness temperature, $^{\circ}K$
X	Terms within the second brace of Equation (5)
Z_F	Geopotential height for FNWC data
$\tilde{Z}_F$	Estimator for geopotential height for NESC data
Z_N	Geopotential height for NESC data
$\tilde{Z}_N$	Estimator for geopotential height for NESC data
$Z(p_j)$	Geopotential height for pressure level p_j
τ	Fractional transmittance
μm	Micrometer
ν_i	Wavenumber for channel i in $(\text{centimeters})^{-1}$

ACKNOWLEDGEMENTS

The author wishes to express his warm appreciation to Professor Frank L. Martin for his generous assistance and guidance in the research and preparation of this paper.

Appreciation is also expressed to the staff of the W. R. Church Computer Facility of the Naval Postgraduate School, and to the Fleet Numerical Weather Central at Monterey.

I. INTRODUCTION

The Satellite Infrared Spectrometer (SIRS-B) carried on the NIMBUS IV spacecraft system relays to National Aeronautics and Space Administration (NASA), at Goddard Space Flight Center, radiance observations taken in seven distinct channels of the 15 μm band of carbon dioxide, and one at 899.0 cm^{-1} in the atmospheric window. In addition, there are six channels in the water-vapor rotational band also being relayed by NIMBUS IV, but these latter six channels will not bear on the subject of this dissertation.

Each of the eight primary channels (699.3 cm^{-1}, 677.8 cm^{-1}, 692.3 cm^{-1}, 699.3 cm^{-1}, 706.3 cm^{-1}, 714.3 cm^{-1}, 750.0 cm^{-1}, and 899.3 cm^{-1}) is sensitive to temperature variations in the tropospheric-stratospheric range of heights. In addition, each channel has a maximum transmissivity in a discrete height range above the surface. Smith, Woolf, and Jacob (1970) presented a graph depicting $d\tau/d\ln p$ versus pressure where τ is the transmissivity and the derivative, $d\tau/d\ln p$, becomes a weight factor of the relative contributions of the various elevations to the total emitted radiance in the channel. It can be seen in Figure 1 and Equation (1), after Smith et al (1970), that the different channel radiances are most responsive to changes in temperature which occur at the level of their peaks in $d\tau/d\ln p$. Each channel tends to signal the occurrence of temperature

changes at or near its own pressure-level peak, as discernible from Figure 1.

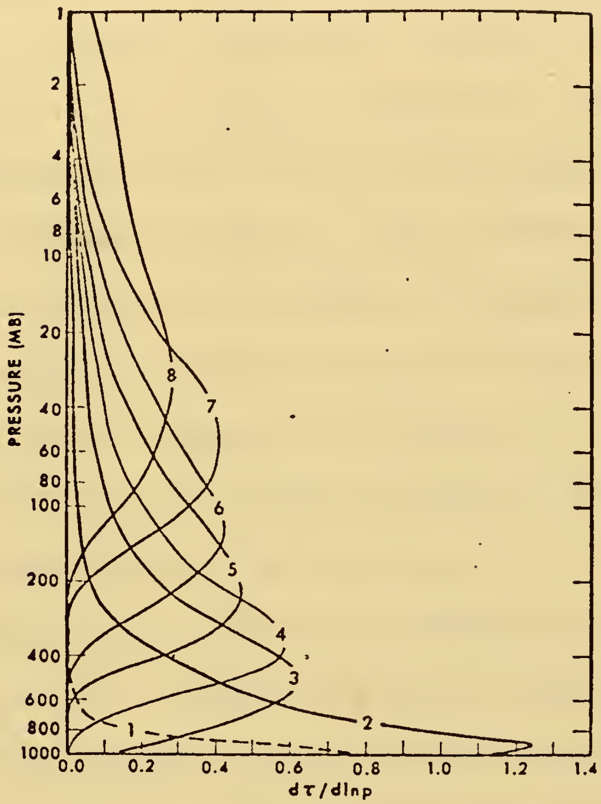

Fig. 1 Derivative of transmittance with respect to the logarithm of pressure for eight SIRS-A channels [after Smith et al (1970)] .

The radiative transfer integral applied to a clear column of air for which the sounding T(p) is known gives the radiance as

$$N(\nu_i) = B\left[\nu_i, T(p_s)\right] \tau(\nu_i, p_s) - \int_{1}^{(p_s)} B\left[\nu_i, T(p)\right] d\tau_i \qquad (1)$$

where $B\left[\nu_i, T(p)\right]$ is the Planck radiance at wave number ν_i. and T(p), the temperature at pressure level p. In

Equation (1) the subscript "s" indicates a surface value and $\tau(\nu_i, p)$ is the fractional transmittance of the atmosphere in the spectral interval centered at ν_i from pressure level p up to the satellite. If the sounding is known, the radiance in the channel centered at wave number ν_i can be computed since $\tau(\nu_i, p)$ is known as a function of pressure p Smith (1970) . The inverse problem has become more relevant since the advent of the SIRS instrument, namely in the use of observations in the eight channels to deduce the clear atmosphere structure $T = T(p)$. The usual method of solving an integral equation for the function $B(\nu_i, T)$ was found to be unstable, but it was found [Smith et al (1970)] that regression methods relating temperatures and geopotential heights at standard pressure levels were quite well described by the results of SIRS scan-soundings

Smith, Woolf, and Jacob (1970) found it convenient to convert the clear column radiances into equivalent "brightness temperatures," $T_B(\nu_i)$. The definition of $T_B(\nu_i)$ is based upon the particular Planck function for temperature $T_B(\nu_i)$ which equals the clear-column channel radiance $N(\nu_i)$, that is

$$B\left[\nu_i, T_B(\nu_i)\right] = N(\nu_i) \qquad (2)$$

so that by solving for T_B we have

$$T_B(\nu_i) = c_2\nu_i \left\{ \ln\left[c_1\nu_i^3/N(\nu_i)\right] + 1 \right\}^{-1} \qquad (3)$$

Here the constants C_1 and C_2 have the values

$$C_1 = 1.19061 \times 10^{-5} \text{ erg-cm}^2\text{-sec}^{-1}\text{-steradian}^{-1} .$$

$$C_2 = 1.43868 \text{ cm-}^{\circ}\text{K}$$

Smith et al (1970) derived regression equations for contour heights at standard pressure levels (see Table 1) utilizing the eight simultaneous brightness temperatures $T_B(\nu_i)$ as independent variables. As dependent variables they employed a large sample of radiosonde-reported geopotential-heights at the mandatory levels. Their results for the month of September, 1969, using a two-week sample, was stated in the nonlinear regression form

$$z(p_j) = \bar{z}(p_j) + \sum_{i=1}^{8} b(\nu_i, p_j) \cdot \left[T_B(\nu_i) - \bar{T}_B(\nu_i)\right] + \sum_{i=1}^{8} b'(\nu_i, p_j) \left[T_B(\nu_i) - \bar{T}_B(\nu_i)\right]^2 \qquad (4)$$

with an analogous regression equation for $T(p_j)$. Their regression coefficients for the September, 1969 SIRS-A example are shown in Table 1, where the coefficients for $T(p_j)$ are also listed. For the data period, 24-29 December 1970, employed in this study, an analogous set of regression equations based upon updated SIRS-climatology would be used.

It is clear that the form in Equation (4), as employed by Smith et al (1970), essentially builds from the temperature structure of the remotely-sensed atmospheric columns with $p_s = 1000$ mb and reconstructs a height profile by

TABLE 1. Height and Temperature Regression Coefficients and Constants for September, 1969 [after Smith et al (1970)]

A. Sample Mean Brightness Temperatures

ν_i(cm^{-1})	899.3	750.0	714.3	706.3	699.3	692.3	677.8	669.3
$\bar{T}_B$(°K)	290.5	273.1	248.1	235.9	226.6	224.2	225.9	233.5

B. Sample Mean Temperature and Temperature Regression Coefficients

P_j	$\bar{T}$(°K)	a_1	a_2	a_3	a_4	a_5	a_6	a_7	a_8	a_1'	a_2'	a_3'	a_4'	a_5'	a_6'	a_7'	a_8'
1,000	292.1	.46	.64	-.10	-1.28	2.01	-2.22	.67	.02	.007	-.021	-.073	.099	-.077	.221	-.202	.157
850	286.0	.16	.50	1.25	-.50	-.50	.22	-1.17	1.03	.005	-.013	-.009	-.180	-.170	.052	.120	.067
700	276.6	.03	.18	1.07	.41	-.65	-.85	-.19	.59	.002	-.008	.001	-.109	-.008	.041	.045	-.022
500	260.2	.02	-.10	.86	.94	-.23	-1.66	.74	.31	-.001	-.009	-.011	.037	.051	-.087	.036	.143
400	248.6	.04	-.28	.89	.78	.94	-2.72	1.15	.26	.005	-.016	-.036	.124	.060	-.118	.048	.120
300	233.2	.04	-.25	.45	.66	2.41	-3.24	.54	.58	.003	-.010	-.019	.112	.272	-.188	.116	-.042
250	225.5	.04	-.12	.12	-.21	4.54	-2.64	-.88	.42	-.005	.012	.033	-.038	.410	-.101	.053	-.259
200	220.7	.04	.04	.07	-1.22	3.78	1.31	-2.44	-.29	-.010	.022	-.014	-.053	-.188	.098	-.003	-.008
150	217.2	.02	.11	-.09	-1.01	.49	3.39	-1.42	-.58	.000	.005	.012	-.075	.067	-.156	.040	.172
100	214.3	-.03	-.07	-.27	-.03	-1.32	2.16	.88	-.44	.003	-.001	.030	-.031	.156	-.045	-.115	.060
50	218.0	-.04	-.24	.36	.36	-.50	.11	1.60	-.49	-.001	.004	-.004	-.039	-.098	.132	-.050	-.070
30	221.7	-.01	-.11	.39	.07	.18	-.36	1.15	-.31	-.001	.005	-.020	-.048	.051	-.011	.085	-.086
10	233.9	-.04	.07	.04	-.13	.50	-.62	-.13	.60	-.001	-.004	.033	-.161	.009	.085	-.072	.061

C. Sample Mean Geopotential Height and Geopotential Height Regression Coefficients

P_j	$\bar{Z}$(m)	b_1	b_2	b_3	b_4	b_5	b_6	b_7	b_8	b_1'	b_2'	b_3'	b_4'	b_5'	b_6'	b_7'	b_8'
1,000	120	-2.74	4.54	-26.12	6.81	-7.50	-27.00	-.81	13.53	.023	-.122	1.990	-1.778	4.783	-2.385	-2.231	1.625
850	1503	-1.04	7.85	-23.14	1.36	-4.21	-29.96	-5.74	19.37	.068	-.196	1.868	-2.191	5.192	-2.751	-1.864	2.315
700	3106	-.46	9.46	-15.67	.55	-7.60	-32.58	-9.01	23.74	.097	-.300	1.780	-2.912	4.555	-2.322	-1.452	2.673
500	5755	-.43	9.38	-6.12	8.38	-12.37	-45.52	-5.58	27.50	.085	-.370	1.589	-3.021	4.522	-2.031	-1.448	3.380
400	7418	-.36	7.89	-.50	15.14	-9.79	-60.66	.32	29.41	.123	-.447	1.383	-2.796	4.480	-2.662	-1.333	4.762
300	9448	-.04	5.83	4.56	22.45	2.90	-84.98	7.01	33.27	.181	-.619	1.335	-1.723	5.167	-3.728	-.993	5.305
250	10671	.07	4.55	5.64	25.19	22.89	-101.14	5.62	36.12	.174	-.597	1.547	-1.935	6.391	-4.589	-.499	4.495
200	12128	.41	4.50	6.10	19.44	52.40	-108.46	-4.78	37.53	.105	-.450	1.459	-1.894	6.926	-4.324	-.375	3.277
150	13973	.64	5.48	6.76	7.47	73.08	-86.61	-22.41	32.64	.060	-.327	1.403	-2.453	6.252	-5.272	1.175	2.978
100	16521	.88	4.72	7.83	-.26	59.63	-44.28	-28.64	26.16	.053	-.210	1.047	-2.665	7.652	-5.214	-.485	5.211
50	20911	.22	2.95	2.99	1.79	34.37	-11.69	-9.86	15.46	.036	-.222	1.820	-2.032	7.995	-5.574	-1.452	5.201
30	24201	-.11	.52	7.55	6.83	30.82	-15.29	14.27	5.90	.054	-.129	1.471	-3.147	7.666	-4.859	-.929	4.187
10	31533	-.17	-.66	17.08	2.71	40.26	-27.91	31.76	5.15	-.058	.339	-.520	-3.850	7.434	-2.421	-1.335	4.179

statistically relating $Z(p_j)$ through the hydrostatic equation to $Z(p_k)$ at any other level desired.

The objective of this study was to obtain statistical relationships for geopotential heights of the 500 mb and 300 mb pressure levels by stepwise regression analysis between these variables and the eight clear-column satellite radiances. Further, it was desired to do this without prior computation of the brightness temperatures. The latter procedure is an unnecessary step if corrected radiances are known, as was the case in this study. If a sixteen-predictor equation were developed, Equation (4) would then be modified to include the N_i and N_i^2 terms $(i = 1,...8)$ with appropriate coefficients.

With the use of NIMBUS IV SIRS-B corrected radiances, N_i, and National Environmental Satellite Center (NESC) regression-computed contour heights at the same geographic locations, diagnostic regression equations for the 500 mb and 300 mb geopotential heights were developed. Separate regression equations were developed using both three-day and four-day pooled data bases. The regression equations developed were tested for validity on an independent sample in each case.

The same procedure was applied to Fleet Numerical Weather Central (FNWC) analyzed geopotential heights at the 500 mb and 300 mb levels for the same positions and times. In the latter case, the contour heights had in no way been related to SIRS-B scan-soundings. Thus, any diagnostic and

prognostic relationships discovered here would have to be based upon the statistical correlation coefficients $R\left[Z(5,3),N_i\right]$, $i = 1,\ldots,8$, as previously suggested by Smith et al.

II. DATA PROCESSING

A. THE ORIGINAL NESC DATA

The original data obtained from the National Environmental Satellite Center (NESC) consisted of a computer listing, by days, of selected SIRS-B scan spots during the period Dec. 1970 - Jan. 1971. Included in this listing were the geographical sites and times of each observation, amounts and heights of effective cloud cover, temperatures and heights of the standard levels, and a double set of radiances. The latter were the original set of uncorrected radiances and the cloud-corrected values for each channel. The uncorrected radiances in the window channel were missing since that channel had become inoperative by December, 1970. The sample of scan-spots presented by NESC was therefore restricted to sites having known surface temperatures so that a realistic effective window channel radiance, $B(\nu, T_s)$ for a surface pressure level $p_s = 1000$ mb could be assigned for each location.

It should be pointed out at this stage that the SIRS-B radiometer carried aboard the NIMBUS IV differed from the SIRS-A radiometer aboard the NIMBUS III in that the SIRS-B radiometer had a "side-looking" capability as well as the vertical mode. This permitted a wider range of soundings in SIRS-B than was possible with SIRS-A. These side-view radiances were normalized to a single atmospheric

emitter-depth located over the scan spot so that all the data was compatible, apart from variations in cloud cover and surface-layer lapse variations.

Because of the scan-spot area of (225 km)^2, most spots viewed were partially cloud-filled with some effective fraction, A. This fact complicated the determination of the cloud-corrected T(p) profiles since the radiances were reduced to

$$\begin{aligned} N(\nu_i) = A \Big\{ & B\left[\nu_i, T_i(p_c)\right] \tau(\nu_i, p_c) \\ & - \int_1^{\tau_c} B\left[\nu_i, T(p)\right] d\tau_i \Big\} \\ + (1 - A) \Big\{ & B\left[\nu_i, T(p_s)\right] \tau(\nu_i, p_s) \\ & - \int_1^{\tau_s} B\left[\nu_i, T(p)\right] d\tau_i \Big\} \end{aligned} \qquad (5)$$

assuming a one-level cloud model with the top at p_c. Here the part of Equation (5) within the second brace is that part of $N(\nu_i)$ which represents the desired uncontaminated radiance in channel i which escapes through the cloud-free fraction, 1 - A.

Smith et al (1970) have outlined a method for determining a cloud-contamination correction which yields the estimate for corrected radiance $N_c(\nu_i)$ in each channel. Since the work in this study was dependent upon the accuracy of the corrected radiances, a brief explanation of this correction

procedure is given, based on the one-level cloud model with top at level p_c. Equation (5) can be broken into two parts,

$$N_c(\nu_i) = N(\nu_i) + C(\nu_i) \tag{6}$$

where the correction $C(\nu_i)$ is designed to eliminate the effects of cloud-reduction of the radiance, and may be obtained by dividing Equation (5) by the factor 1-A. However, this will not be a permissible procedure since the cloud cover, A, may be very close to unity. Instead, Smith et al (1970) suggest an iterative procedure whereby $C(\nu_i)$ of Equation (6) may be obtained in the form

$$C(\nu_i) = A\left\{N_c(\nu_i) - X\left[\nu_i, p_c, T(p)\right]\right\} \tag{7}$$

The function $X\left[\nu_i, p_c, T(p)\right]$ represents the contents of the second brace of Equation (5). Successive corrections $C(\nu_i)$ are then determined for each channel 4,....,8, by making the assumption that the radiances observed in channels 2 and 3 (750.0 cm^{-1} and 714.0 cm^{-1}) are correct during iterations while correcting the remaining set of radiances $N_4,\ldots N_8$.

In determining a first guess to a clear column atmosphere T(p) the five most opaque channels in Figure 1 are assumed correct at the first iteration, as well as the predetermined window channel. The NESC correction scheme then makes use of a six-predictor regression equation for T(p) (analogous to Equation (4) but lacking channel 2 and 3 terms)

which then specifies the required first guess $T(p_j)$ at all standard levels. With this profile now specified the best-fit consistent choices of A, 1-A, and p_c which comes closest to providing the best-fit solutions $N(\nu_i)$ to Equation (5) for channels 2 and 3 are obtained. In this test p_c is subject to variation over the standard levels $p = 200, 250, \ldots 850$ mb and the best-fit A, 1-A, are thereby chosen. At each iteration, there is an improved set of six corrected radiances, which leads to an improved specification $T(p_j)$. This then leads to improved newly corrected radiances $N_c(\nu_i)$ $(i = 4, \ldots, 8)$ in accord with Equations (6) and (7). Finally, in a limited number of iterations $C(\nu_i)$ approaches a convergent value. At this final stage, the six-predictor regression equation for $T(p_j)$ gives estimates of corrected radiances in channels 2 and 3. The listed statistics relating p_c and A are of no particular importance since these quantities relate only to an effective cloud cover over an area $(225 \text{ km})^2$, and the cloud-depth is considered irrelevant in obtaining $N_c(\nu_i)$. The important factor to be tested in this paper is the concept that geopotential heights as taken from a large radiosonde sample are highly correlated with the set of clear-column radiances, i.e., to the estimated $T(p)$ structure of the atmosphere. Thus the NESC SIRS-B data obtained by the December 1970 version of the NESC regression equation system provided also the geopotential heights and

temperatures at all standard levels in the atmosphere from p = 1000 mb to 10 mb.

In developing the NESC regression equations, Smith et al (1970) utilized a data sample of approximately two weeks, continually updating the sample period closer to the time when the independent calculations were made. The heights used in their regression equations were interpolated in space and time from National Meteorological Center analyzed fields at standard pressure levels to the geographical locations and observed times of the SIRS measurements. Only portions of analyses and NIMBUS III data close to radiosonde observations were used for developing their dependent data regression coefficients giving heights from corrected radiances. These NESC dependent samples were divided into latitude bands (18-40°N, 35-55°N, and 50-80°N). A similar technique was used by NESC in making available the data from December 1970, a portion of which was used in this thesis. This data consisted of corrected radiances at scan-spots which were used in conjunction with an eight-predictor regression equation for generating temperature and height values for the standard levels from the SIRS observations. These computed heights and temperatures appeared on the NESC data listings for 24-28 December 1970, which were used in this study.

The NESC regression-derived heights of the 500 mb and 300 mb levels, position, time, and clear-column radiances for each sounding from 24-27 December, 1970, were used for the regression analysis described in Chapter III.

B. FNWC DATA

Height fields for 0000 GMT and 1200 GMT covering the period 24-29 December 1970, were obtained from the data-tapes of Fleet Numerical Weather Central (FNWC) at Monterey for both the 500 mb and 300 mb levels. The contour heights were interpolated in space and time to the same positions and times of the satellite data obtained from NESC. The spatial values of geopotential height were computed by use of a double-quadratic Bessel interpolation scheme applied to both the synoptic times preceding and following each satellite observation. Then the heights were interpolated linearly to the time of the satellite observation. The computer program used to accomplish the interpolation scheme is listed in the Appendix.

The FNWC data provided an independent set of geopotential heights for the 500 mb and 300 mb levels from which a second set of regression relations could be derived for comparison with the regression analyses performed on the NESC data.

III. DEPENDENT DATA REGRESSIONS

A. DEVELOPMENT OF REGRESSION EQUATIONS USING NESC GENERATED VALUES OF 500 MB AND 300 MB GEOPOTENTIAL HEIGHTS.

The NESC-generated 300 mb and 500 mb pressure levels ($Z_N(5)$ and $Z_N(3)$ respectively) were selected for investigation with the corresponding 500 mb and 300 mb FNWC analyses, which presently have no SIRS input. A multiple linear regression analysis technique was used in this study corresponding to the 8-predictor scheme of Smith, Woolf, and Jacob (1970), but containing no nonlinear terms. The specific program used was BIMED 02R, a version of the stepwise linear regression technique currently on file at the Statistical Library of the W. R. Church Computer Facility at the Naval Postgraduate School, after Dixon (1966). The result of this technique when applied to simultaneous data samples of the form $[Z_i, N_1, N_2, .., N_8]$ is to produce regression equations of the form

$$Z = C_o + \sum_{i=1}^{8} C_i N_i = (C_o, C_1, \ldots, C_8) \begin{pmatrix} 1 \\ N_1 \\ N_2 \\ \cdot \\ \cdot \\ \cdot \\ \cdot \\ \cdot \\ \cdot \\ N_8 \end{pmatrix} \qquad (8)$$

Here the subscripts 1,..,8 indicate the channel numbering system and are also used for variable numbering. A series of dependent test regressions were performed on both $Z_N(5)$

and $Z_N(3)$ using a pooled three-day data base and a pooled four-day data base of simultaneous values of SIRS-B corrected radiances. Due to the nature of the data available, each data-day presented a composite of scan-soundings centered about 1200 GMT, varying up to six hours on either side of this central time. The data was further divided into three overlapping latitude bands. The limits of each band are listed below:

Band 1	20°N - 40°N
Band 2	35°N - 55°N
Band 3	50°N - 70°N

The resulting coefficients (C_0, C_1,....,C_8) for the three-day and four-day regression equations are listed in Tables 2 and 3 for the 500 mb and 300 mb dependent tests, respectively.

TABLE 2. 500 mb NESC Dependent Regression Coefficients for Three- and Four-Day Data Base, Giving Best-fit for Eq. (8)

3-Day Sample Base

Sample Size	Band 1 171	Band 2 190	Band 3 177
C_0	5473.77	5689.80	4620.48
C_1	6.66	-2.80	-2.90
C_2	-17.56	-3.32	-11.68
C_3	23.85	41.83	62.59
C_4	28.06	-10.83	-17.87
C_5	-62.22	-66.78	-36.90
C_6	-6.80	4.02	-4.14
C_7	21.20	19.62	11.74
C_8	-0.33	-1.40	*

4-Day Sample Base

Sample Size	Band 1 171	Band 2 227	Band 3 216
C_0	5497.55	5756.70	4555.32
C_1	6.53	-1.18	-4.45
C_2	-15.98	-7.75	-6.38
C_3	20.13	45.24	54.55
C_4	34.33	-12.75	-10.93
C_5	-67.57	-64.77	-35.75
C_6	-5.88	2.64	-7.94
C_7	24.18	19.54	1.00
C_8	-3.26	-1.13	1.45

*Indicates an insignificant contribution to the analysis of variance by this predictor.

TABLE 3. 300 mb NESC Dependent Regression Coefficients for Three- and Four-Day Data Base, Giving Best Fit for Eq. (8)

3-Day Sample Base

Sample Size	Band 1 171	Band 2 190	Band 3 177
C_o	8976.59	8490.63	7166.52
C_1	12.79	4.00	1.57
C_2	-22.36	-6.08	-15.54
C_3	4.04	21.62	54.11
C_4	87.54	47.07	23.71
C_5	-105.20	-96.10	-48.47
C_6	-15.77	4.64	-4.34
C_7	23.90	15.88	6.14
C_8	5.67	1.62	1.29

4-Day Sample Base

Sample Size	Band 1 206	Band 2 227	Band 3 216
C_o	8986.32	8613.84	7102.40
C_1	13.26	6.65	*
C_2	-21.76	-13.75	-10.18
C_3	*	29.09	45.98
C_4	95.49	41.53	30.92
C_5	-110.81	-93.15	-47.49
C_6	-14.34	3.13	-8.48
C_7	28.03	16.26	5.37
C_8	1.25	1.65	2.94

*Indicates an insignificant contribution to the analysis of variance by this predictor.

The coefficients in Tables 2 and 3 are considerably different in each latitude band which tends to justify the use of separate latitude bands in the analyses. Whether the limits of each latitude band are optimum or not is undetermined, but it was felt that any further reduction in the width of each band would reduce the number of soundings used in each regression equation and thereby have a detrimental effect on a statistical analysis. The differences between the corresponding coefficients from the three- and four-day sample regressions were generally insignificant; however, this conclusion will be further tested by examination of the fractional explainted variance accounted for by the appropriate regression equations when applied to the data-samples.

In both Tables 2 and 3, the coefficients corresponding to channels 3, 4, and 5 appear to be weighted more heavily than any other triad of coefficients, which appears to be consistent with the response levels of Figure 1.

A useful statistic for the fractional unexplained variance is

$$1 - R^2 = \frac{n - k - 1}{n - 1} \left(\frac{\text{std. error}}{\text{std. dev.}} \right)^2 \tag{9}$$

where k is the number of predictors and n the sample size.

Thus the fractional explained variance is easily obtained from Equation (9) as

$$R^2 = 1 - \frac{n - k - 1}{n - 1} \left(\frac{\text{std. error}}{\text{std. dev.}} \right)^2 \qquad (10)$$

Values for R^2 and of standard errors for each of the dependent tests corresponding to Tables 2 and 3 are listed in Table 4.

TABLE 4. R^2 and Standard Errors (gpm) for NESC Dependent Regression Equations for 500 mb and 300 mb Three- and Four-day samples.

500 mb

3-Day Sample	Band 1	Band 2	Band 3
R^2	.8050	.8222	.9050
Std. error(m)	61.72	77.13	69.68
4-Day Sample			
R^2	.8039	.8154	.9051
Std. error(m)	60.55	76.78	69.79

300 mb

3-Day Sample	Band 1	Band 2	Band 3
R^2	.8790	.8693	.9351
Std. error(m)	77.51	91.80	75.36
4-Day Sample			
R^2	.8764	.8622	.9349
Std. error(m)	76.22	91.42	75.50

As indicated in Table 4, Band 3 appears to produce higher values for R^2, and therefore better results, than the other two bands in the NESC dependent regression analysis. The standard errors for the 300 mb tests were generally higher than the 500 mb tests, but one might expect this to happen since the standard deviations of $Z_N(3)$ are greater than those of $Z_N(5)$. In general, the 300 mb tests gave higher values of R^2 upon specification than the corresponding 500 mb tests.

B. DEVELOPMENT OF REGRESSION EQUATIONS USING FNWC-INTERPOLATED VALUES OF 500 MB AND 300 MB GEOPOTENTIAL HEIGHTS.

Procedures similar to those used in Part A of this chapter were used on the FNWC 500 mb and 300 mb geopotential heights [$Z_F(5)$ and $Z_F(3)$ respectively] , corresponding to the identical SIRS scan-sounding positions and times. The same latitude band limits as specified in III.A. were used for both the three- and four-day regression analyses. The resulting coefficients for the FNWC regression equations are listed in Tables 5 and 6 for the 500 mb and 300 mb dependent tests, respectively.

TABLE 5. 500 mb FNWC Dependent Regression Coefficients for Three- and Four-day Data Base

3-DAY SAMPLE BASE

Sample Size	Band 1 171	Band 2 190	Band 3 177
C_o	5617.09	5583.51	4615.09
C_1	7.58	-2.25	-2.50
C_2	-19.82	-2.58	-9.43
C_3	23.50	38.35	57.19
C_4	25.55	-6.14	-16.06
C_5	-53.38	-67.11	-32.17
C_6	-13.71	5.85	-9.10
C_7	23.14	19.19	12.22
C_8	-1.35	-2.37	0.80

4-DAY SAMPLE BASE

Sample Size	Band 1 206	Band 2 227	Band 3 216
C_o	5653.75	5762.27	4595.81
C_1	7.70	0.36	-2.24
C_2	-20.43	-10.14	-9.16
C_3	24.21	46.38	55.72
C_4	28.86	-13.41	-15.03
C_5	-59.44	-64.52	-30.50
C_6	-12.29	4.74	-9.58
C_7	27.24	19.12	8.71
C_8	-5.01	-2.15	3.26

TABLE 6. 300 mb FNWC Dependent Regression Coefficients for Three- and Four-day Data Base

3-DAY SAMPLE BASE

	Band 1	Band 2	Band 3
Sample Size	171	190	177
C_o	9156.82	8451.37	7337.29
C_1	14.03	2.99	*
C_2	-33.45	-8.12	-18.36
C_3	28.34	34.19	71.49
C_4	50.39	29.29	-3.58
C_5	-72.67	-86.77	-35.32
C_6	-29.22	5.55	-9.36
C_7	21.93	15.05	9.18
C_8	8.82	0.78	*

4-DAY SAMPLE BASE

	Band 1	Band 2	Band 3
Sample Size	206	227	216
C_o	9226.42	8702.09	7289.23
C_1	15.01	7.09	*
C_2	-36.75	-20.98	-16.37
C_3	31.79	49.50	66.94
C_4	52.29	16.47	*
C_5	-77.84	-83.39	-33.79
C_6	-27.24	4.64	-9.98
C_7	26.96	15.72	5.07
C_8	3.44	0.41	2.85

*Indicates an insignificant contribution to the analysis of variance by this predictor.

The FNWC regression coefficients listed in Tables 5 and 6 lend support to the observations from the NESC regression coefficients, in that the coefficients from the FNWC dependent test vary sufficiently between latitude bands to justify using separate bands. Furthermore, the differences between the three-day samples and four-day samples are again small; and the coefficients corresponding to Channels 3, 4, and 5 appear to be weighted more heavily than the others.

Table 7 lists the values for R^2 and standard errors for each of the FNWC dependent tests listed in Tables 5 and 6. As in the NESC tests, the values for R^2 were higher in Band 3, standard errors were generally larger for the 300 mb tests than for the 500 mb tests, and the values for R^2 were higher for the 300 mb tests than for the 500 mb tests. A comparison of the three- and four-day sample regressions for both the 300 mb and 500 mb cases revealed no significant differences in corresponding values of R^2, when subjected to to a t-test.

TABLE 7. R^2 and Standard Errors (gpm) for FNWC Dependent Regression Equations for 500 mb and 300 mb Three- and Four-day Dependent Samples.

500 mb

3-Day Sample	Band 1	Band 2	Band 3
R^2	.7910	.7954	.9014
Std. error(m)	62.53	84.55	72.48
4-Day Sample			
R^2	.7787	.7899	.8989
Std. error(m)	63.79	83.69	73.21

300 mb

3-Day Sample	Band 1	Band 2	Band 3
R^2	.8575	.8361	.9235
Std. error(m)	84.38	105.99	84.32
4-Day Sample			
R^2	.8459	.8328	.9222
Std. error(m)	85.77	104.26	85.07

C. COMPARISONS BETWEEN NESC AND FNWC DEPENDENT REGRESSION ANALYSES

If one compares the results from Tables 2, 3, 5, and 6, channels 3, 4, and 5 appear to be weighted more heavily than the other channels for both the NESC and FNWC dependent tests. Table 8 combines the results of Tables 4 and 7 to facilitate comparison of NESC and FNWC dependent regression test results. Here, only comparative values of R^2 by the various dependent stratifications are considered. If standard errors are required, reference should be made to Tables 4 and 7.

Band 3 gave the highest values of R^2, averaging 8.7% higher over all dependent regression systems than Bands 1 and 2, varying from 5.6% to 12.0% higher for individual comparisons. The 300 mb values of R^2 averaged 4.65% higher overall than the 500 mb values of R^2. with the NESC 300 mb values of R^2 averaging 5.01% higher than the NESC 500 mb values, and the FNWC 300 mb values of R^2 averaging 4.38% higher than the FNWC 500 mb values.

Although quite close in most instances, in all cases the NESC values of R^2 were slightly higher than the corresponding values of R^2 from the FNWC tests, averaging 2.01% higher for the NESC tests. A closer look reveals an average of 1.69% smaller values, or "shrinkage," for the FNWC 500 mb tests as compared to the corresponding NESC tests. An average shrinkage of 2.32% occurred for the 300 mb FNWC tests as compared to the NESC tests. The individual

TABLE 8. Summary of NESC and FNWC Dependent Regression Test Results.

	NESC 500 mb				FNWC 500 mb				
	Band 1	Band 2	Band 3	Average	Band 1	Band 2	Band 3	Average	Avg.
3-Day	.8050	.8222	.9050	.8441	.7910	.7954	.9014	.8293	.8367
4-Day	.8039	.8154	.9051	.8415	.7787	.7899	.8989	.8225	.8320
Avg 500	.8045	.8188	.9051	.8428	.7849	.7927	.9002	.8259	.8348
	NESC 300 mb				FNWC 300 mb				
	Band 1	Band 2	Band 3	Average	Band 1	Band 2	Band 3	Average	Avg.
3-Day	.8790	.8693	.9351	.8945	.8575	.8361	.9235	.8724	.8835
4-Day	.8764	.8622	.9349	.8912	.8459	.8328	.9222	.8670	.8791
Avg 300	.8777	.8658	.9350	.8929	.8517	.8345	.9229	.8697	.8813
Average 500+300	.8411	.8423	.9201	.8679	.8183	.8136	.9116	.8478	.8579

shrinkages of R^2 for each band, averaged over both the three- and four-day data-samples is shown for the FNWC tests relative to the NESC corresponding tests:

	Band 1	Band 2	Band 3
500 mb	1.96%	2.61%	0.49%
300 mb	2.60%	3.13%	1.21%

Bands 3 shows the smallest shrinkage of R^2 values for FNWC as compared to the NESC dependent tests. That the NESC values of R^2 are higher than the FNWC values is not too surprising since the NESC data was originally the result of essentially an eight-predictor equation, the precise form of which was not known in this study.

A comparison of three- and four-day overall regression systems showed that the three-day values of R^2 were .46% higher than the four-day values. Since this is such a small difference, it is likely to be caused only by the additional data samples used in converting the particular three-day sample to a four-day sample, and the difference was not considered significant.

Thus far, it is seen from the dependent-data tests on NESC and FNWC samples that the results are generally good, considering the R^2 values averaged .8579, with averages of .8679 for NESC and .8478 for FNWC. From the paragraphs preceding this one, it appears that the dependent tests produced better results in Band 3 than the other bands,

better results at 300 mb than at 500 mb and better results for NESC than for FNWC specification.

It should be pointed out that the NESC and FNWC height data were highly correlated. The 500 mb values of R^2 ranged from .9267 to .9699 and the standard errors varied from 35.26 meters to 43.15 meters. The values of R^2 for the 300 mb case ranged from .9244 to .9707 and the standard errors varied from 51.46 meters to 59.64 meters.

IV. INDEPENDENT SAMPLE TESTS

A. VERIFICATION PROCEDURE FOR THE INDEPENDENT DATA TESTS

Each of the dependent regression equations, stratified by NESC and FNWC, by latitude bands, and for the different sizes of data-bases in Chapter III, was tested using independent data samples. The equations developed from the three-day samples were tested with independent data from a fourth day, for times centered at 12 hours and 24 hours later. The regression equations developed from the four-day samples were likewise tested for times centered 12 and 24 hours later using the equations developed from data collected over 24-27 December, 1970. The corresponding four-day independent tests utilized data from the 28th (28/00 GMT and 28/12 GMT, i.e., 12 and 24 hours later). In addition, the 12- and 24-hour tests provided homogeneous statistics and were pooled to provide a larger number of independent data samples for each band and height.

The results of the independent tests generate equations of the general form

$$Z_N(5,3) = D_o + D_1\tilde{Z}_N(5,3) \qquad (11)$$

and

$$Z_F(5,3) = F_o + F_1\tilde{Z}_F(5,3) \qquad (12)$$

where $\tilde{Z}_N(5,3)$ and $\tilde{Z}_F(5,3)$ represent the height-estimators from the regression equation (Equation 8), D_o and F_o are regression constants, and D_1 and F_1 the regression

coefficients. $Z_F(5,3)$ are the observed independent-test heights determined by interpolation from the data tapes of FNWC for the 500 mb and 300 mb levels. All independent $Z_N(5,3)$ were the result of application of the NESC update regression to the independent set of scan-spot corrected radiances. Regression analyses for these tests were similar to the regression techniques applied in Chapter III, in that the newly computed height $\tilde{Z}$ is now being compared by regression methods to the known height at each scan-sounding location. The independent test results are presented in a slightly different manner in Tables 9, 10, 11, and 12. The mean and standard deviation for the NESC and FNWC verifications, and the values for R^2 and standard error resulting from $\tilde{Z}_N(5)$, $\tilde{Z}_N(3)$, $\tilde{Z}_F(5)$, and $\tilde{Z}_F(3)$ are listed in Tables 9, 10, 11, and 12 for the three- and four-day independent tests.

TABLE 9. Verification Resulting From the Use of Equation (8) Upon 500 mb NESC Independent Data.

3-DAY TEST

		Sample Size	Mean	Std. Dev.	R^2	Std. Error
Band 1	12 hr	23	5753.26	99.04	.7983	45.52
	24 hr	35	5738.60	121.72	.7867	57.07
	12+24 hr	58	5744.41	112.59	.7852	52.64
Band 2	12 hr	31	5464.45	100.76	.5428	69.30
	24 hr	37	5477.38	154.80	.7652	76.08
	12+24 hr	68	5471.48	132.15	.6934	73.62
Band 3	12 hr	32	5283.97	215.61	.8781	76.54
	24 hr	39	5293.51	227.12	.9015	72.24
	12+24 hr	71	5289.21	220.49	.8859	75.01

4-DAY TEST

		Sample Size	Mean	Std. Dev.	R^2	Std. Error
Band 1	12 hr	28	5760.27	90.95	.7537	46.00
	24 hr	57	5739.58	121.90	.8308	50.59
	12+24 hr	85	5746.36	112.52	.8151	48.67
Band 2	12 hr	33	5513.99	140.14	.7093	76.77
	24 hr	50	5432.87	164.26	.7499	83.00
	12+24 hr	83	5465.11	159.32	.7509	80.00
Band 3	12 hr	26	5290.45	202.12	.7685	99.26
	24 hr	47	5286.16	172.66	.8281	72.38
	12+24 hr	73	5287.69	182.30	.7959	82.94

TABLE 10. Verification Resulting from the Use of Equation (8) Upon 300 mb NESC Independent Data.

3-DAY TEST

		Sample Size	Mean	Std. Dev.	R^2	Std. Error
Band 1	12 hr	23	9427.13	166.40	.8980	54.39
	24 hr	35	9398.46	190.90	.8526	74.40
	12+24 hr	58	9409.82	180.62	.8658	66.76
Band 2	12 hr	31	8941.29	157.58	.7172	85.23
	24 hr	37	8981.95	202.08	.8027	91.04
	12+24 hr	68	8963.41	182.96	.7704	88.34
Band 3	12 hr	32	8682.44	293.24	.9084	90.23
	24 hr	39	8695.46	303.44	.9334	79.33
	12+24 hr	71	8689.59	296.83	.9207	84.19

4-DAY TEST

		Sample Size	Mean	Std. Dev.	R^2	Std. Error
Band 1	12 hr	28	9418.45	160.38	.8348	66.42
	24 hr	57	9409.62	203.85	.8718	73.64
	12+24 hr	85	9412.46	189.70	.8615	71.03
Band 2	12 hr	33	9012.87	206.88	.7994	94.15
	24 hr	50	8923.04	234.25	.8137	102.15
	12+24 hr	83	8958.68	226.81	.8148	98.22
Band 3	12 hr	26	8696.30	266.23	.8301	111.99
	24 hr	47	8696.93	242.90	.8827	84.13
	12+24 hr	73	8696.62	249.60	.8603	93.94

TABLE 11. Verification Resulting From the Use of Equation (8) Upon 500 FNWC Independent Data.

3-DAY TEST

		Sample Size	Mean	Std. Dev.	R^2	Std. Error
Band 1	12 hr	23	5736.63	91.62	.7572	46.21
	24 hr	35	5724.33	130.80	.7103	71.46
	12+24 hr	58	5729.20	116.11	.7130	62.75
Band 2	12 hr	31	5468.17	123.09	.6163	77.56
	24 hr	37	5473.50	159.20	.7401	82.31
	12+24 hr	68	5471.07	142.86	.6950	79.49
Band 3	12 hr	32	5275.86	208.00	.8440	83.52
	24 hr	39	5291.72	229.58	.8863	78.45
	12+24 hr	71	5284.57	218.72	.8627	81.62

4-DAY TEST

		Sample Size	Mean	Std. Dev.	R^2	Std. Error
Band 1	12 hr	28	5750.87	80.03	.8329	33.34
	24 hr	57	5728.56	120.04	.8054	53.43
	12+24 hr	85	5735.90	108.52	.8104	47.53
Band 2	12 hr	33	5522.73	144.47	.6730	83.94
	24 hr	50	5427.71	171.16	.7143	92.43
	12+24 hr	83	5465.49	166.85	.7170	89.31
Band 3	12 hr	26	5280.39	198.52	.6612	117.93
	24 hr	47	5274.83	180.50	.7782	85.95
	12+24 hr	73	5276.81	185.76	.7297	97.26

TABLE 12. Verification Resulting From the Use of Equation (8) Upon 300 mb FNWC Independent Data.

3-DAY TEST

		Sample Size	Mean	Std. Dev.	R^2	Std. Error
Band 1	12 hr	23	9396.04	160.42	.8465	64.34
	24 hr	35	9378.17	195.55	.7643	96.36
	12+24 hr	58	9385.25	181.16	.7883	84.10
Band 2	12 hr	31	8934.96	187.09	.7281	99.23
	24 hr	37	8975.52	217.55	.7903	101.03
	12+24 hr	68	8957.03	203.76	.7673	99.04
Band 3	12 hr	32	8665.11	282.86	.8915	94.70
	24 hr	39	8694.04	308.89	.9157	90.88
	12+24 hr	71	8681.00	295.70	.9022	93.13

4-DAY TEST

		Sample Size	Mean	Std. Dev.	R^2	Std. Error
Band 1	12 hr	28	9410.61	144.12	.7820	68.57
	24 hr	57	9392.98	200.90	.8310	83.34
	12+24 hr	85	9398.79	183.45	.8198	78.34
Band 2	12 hr	33	9005.81	217.27	.7295	114.81
	24 hr	50	8913.67	244.64	.7718	118.07
	12+24 hr	83	8950.30	237.16	.7641	115.91
Band 3	12 hr	26	8678.84	267.39	.7858	126.31
	24 hr	47	8679.63	257.69	.8367	104.31
	12+24 hr	73	8679.34	259.33	.8188	111.18

B. SUMMARY OF INDEPENDENT TEST RESULTS

1. Results Internal to the Independent Test

Table 13 lists the combined 12 and 24 hour independent-test values of R^2 abstracted from Tables 9, 10, 11, and 12 to facilitate comparisons of test-methods contained in those tables. Again our emphasis is on R^2 as a measure of the efficiency of the verification since this statistic has the effect of normalizing the variable standard deviations in Tables 9, 10, 11, and 12.

Band 3, as in the dependent tests, gave the highest values of R^2, averaging 6.99% higher than the other bands. The 300 mb values of R^2, again, as in the dependent cases, were higher than the 500 mb values, averaging 5.83% higher. The NESC values of R^2, as compared to the FNWC values of R^2, were higher, as before, by an average of 3.60% over all of the independent tests. However, the amount of shrinkage between the NESC and FNWC within the independent tests was a minimum in Band 2, as compared to the minimum values of shrinkage in Band 3 for dependent tests. This phenomenom is due to the fact that the independent test of ${R_N}^2$ fell off considerably in Band 2, whereas the corresponding shrinkage was somewhat less with FNWC independent tests in Band 2. The three-day estimator tests produced average values of R^2 that were .76% higher than the corresponding four-day values for R^2. This, again, as in the dependent tests, is a small difference and is considered to be due to the small sample-size, or to the particular data-sample added to obtain the

TABLE 13. Summary of NESC and FNWC Independent Regression Test Results Using Equation (8).

	NESC 500 mb				FNWC 500 mb				
	Band 1	Band 2	Band 3	Average	Band 1	Band 2	Band 3	Average	Avg.
3-Day	.7852	.6939	.8859	.7882	.7130	.6950	.8627	.7569	.7726
4-Day	.8151	.7509	.7959	.7873	.8104	.7170	.7295	.7524	.7698
Avg 500	.8002	.7224	.8409	.7878	.7617	.7060	.7961	.7547	.7712
	NESC 300 mb				FNWC 300 mb				
	Band 1	Band 2	Band 3	Average	Band 1	Band 2	Band 3	Average	Avg.
3-Day	.8658	.7704	.9207	.8523	.7883	.7673	.9022	.8193	.8358
4-Day	.8615	.8148	.8603	.8455	.8198	.7641	.8188	.8009	.8232
Avg 300	.8637	.7926	.8905	.8489	.8041	.7657	.8605	.8101	.8295
Average 500+300	.8320	.7572	.8657	.8184	.7829	.7359	.8283	.7824	.8004

four-day sample, and therefore of little statistical significance.

2. Comparison of Independent- With Dependent-Data Specification.

From the independent tests, the same basic conclusions as for the dependent tests are to be drawn since the results are quite similar. The independent-test values of R^2 were generally good with an average of .8004, an average of .8184 for R^2 from the independent NESC tests and an average of .7824 for the FNWC tests. The highest values of R^2 were in Band 3, highest at 300 mb, and highest for the NESC tests.

In proceeding from the dependent tests to the independent tests, some loss of accuracy is to be expected. Values of R^2 again will be used for comparisons. Table 14 is derived from Tables 8 and 13 to present an easier comparison of the corresponding values of R^2 from the dependent tests and the independent tests, with the value of shrinkage indicated also. In most cases the shrinkage of the R^2 values from the FNWC dependent tests to the independent tests was slightly larger than the shrinkage for the similar NESC tests. The FNWC shrinkage averaged 1.59% more than the NESC shrinkage.

The first group of numbers in Table 14 are averaged over all bands and over both three- and four-day coefficient estimators. In this group, the values of R^2 for

the NESC 300 mb tests show the lowest relative shrinkage of the four shown in the group. This might have been expected since the 300 mb NESC test results from both the dependent and independent tests showed better results than the others.

The second group of numbers in Table 14 is averaged over the 500 mb and 300 mb level independent tests, and over three- and four-day coefficient estimators $\tilde{Z}$. This second group shows relatively small shrinkages in Band 1. This could possibly be due to the fact that in low latitudes, the radiance correction procedure is somewhat more consistent than in mid-latitudes, and may be affecting the amount of shrinkage in a favorable manner.

The third group of numbers in Table 14 is averaged over all three latitude bands, and shows the relative shrinkages by use of the Equation (8) based upon the three- and four-day dependent coefficient matrices. The amount of shrinkage of the three-day independent tests over the four-day tests, or vice-versa, is not very obvious, even though one might expect that the four-day tests should be more representative due to a larger input of data. From the findings of this study, it has consistently been determined that tests on independent data using the four-day data-base estimators are on the average slightly less effective in R^2 than when the corresponding three-day data base was used.

TABLE 14. Summary of Dependent to Independent Test Shrinkage.

Test Being Compared	Dependent Value of R^2	Independent Value of R^2	Average Shrinkage
$Z_N(5)$	.8428	.7878	5.50%
$Z_F(5)$	.8259	.7547	7.12%
$Z_N(3)$	.8929	.8489	4.40%
$Z_F(3)$	.8697	.8101	5.96%
			avg. 5.75%
Z_N Band 1	.8411	.8320	.91%
Z_F Band 1	.8183	.7829	3.54%
Z_N Band 2	.8423	.7572	8.51%
Z_F Band 2	.8136	.7359	7.77%
Z_N Band 3	.9201	.8657	5.44%
Z_F Band 3	.9116	.8283	8.33%
			avg. 5.75%
$Z_N(5)$ 3-day	.8441	.7882	5.59%
$Z_N(5)$ 4-day	.8415	.7873	5.42%
$Z_N(3)$ 3-day	.8945	.8523	4.22%
$Z_N(3)$ 4-day	.8912	.8455	4.57%
$Z_F(5)$ 3-day	.8293	.7569	7.24%
$Z_F(5)$ 4-day	.8225	.7524	7.01%
$Z_F(3)$ 3-day	.8724	.8193	5.31%
$Z_F(3)$ 4-day	.8670	.8009	6.61%
			avg. 5.75%

V. CONCLUSIONS

It has been shown in this study that regression equations developed from relatively small data bases of heights and corrected SIRS-B radiances can be used to compute heights on independent samples with relatively good results. It is felt that further testing should be conducted at other levels using comparisons of other samples to test the results obtained here. If the resources are available, larger data bases should be tested in a similar manner. Direct application of similar procedures could be of possible use in the update of FNWC analyses for standard levels in areas of sparse data, or even aboard ships with weather offices to provide real-time height calculations over an operational area. In the latter case the advantage of a small data base lies in the relatively small amount of core storage necessary for the type of computer calculations possible in shipboard operations.

Although the NESC height data provided slightly better regression results than the FNWC height data, this was to be expected since the NESC heights were computed using an eight-predictor regression equation, and therefore were internally more consistent. The results obtained by using FNWC data for dependent and independent regression analyses, paralleling the procedures applied to the NESC data, lends support

to the overall concept of developing regression equations to compute geopotential heights using SIRS-B corrected radiances.

Improvements of the results should be expected if longer-term data samples are used. Improvements should also be expected if the width of the latitude bands were smaller, and if the radiance data were subjected to gross error checks before entering into regression analyses. Also, a fact to be considered is the tendency of the SIRS-B channel response to degrade and require updated calibration after being in orbit for a period of time. If degradation errors were linear in time, the regression-climatology should provide update corrections, but the normal case is that degradation occurs non-uniformly in the different channels. The best scan-soundings are normally obtained soon after the satellite is launched into its orbit about the earth, before appreciable system-degradation can occur.

APPENDIX

GRIDDING AND INTERPOLATION SCHEME

```
      DIMENSION HT00HR(63,63,2),HT12HR(63,63,2),HT24HR(63,63,2),F(63,63)
     1,F1(4),F2(4),F3(4),FP(200),FS(4),FNWC(2)
C     K=1  MEANS THE 500 MB CALCULATIONS ARE BEING PERFORMED
C     K=2  MEANS THE 300 MB CALCULATIONS ARE BEING PERFORMED
      DO 15 K=1,2
      READ(5,77) ((HT00HR(I,J,K),J=1,63),I=1,63)
      READ(5,77) ((HT12HR(I,J,K),J=1,63),I=1,63)
      READ(5,77) ((HT24HR(I,J,K),J=1,63),I=1,63)
   77 FORMAT(13F6.1)
   15 CONTINUE
C
C
C     L=NUMBER OF SOUNDINGS BEING UTILIZED IN THIS GRIDDING AND INTERPOLATIONS.
      L=86
      NUMBER=1
      DO 88 N=1,L
      READ(5,101) IMO,IDA,KTIME1,KTIME2,FLAT,FLONG
  101 FORMAT(I2,1X,I2,1X,2I2,26X,F4.1,4X,F6.1,27X,I3)
      READ(5,102)HT1,HT1
  102 FORMAT(20X,F4.0,6X,F4.0)
      READ(5,103) CH1
  103 FORMAT(3X,F5.2)
      ITIME=KTIME1*100 + KTIME2
      PI=3.141593
      IF(FLONG.LT.0.0) FLONG=FLONG + 360.0
      Y=350.-FLONG
      Y=Y*PI/180.
      ELAT=FLAT*PI/180.
      X=ELAT
      A=1.0 - SIN(X)
      B=1.0 + SIN(X)
      T=A/B
      GRIDI=32.0 + 31.205*SQRT(T)*COS(Y)
      GRIDJ=32.0 + 31.205*SQRT(T)*SIN(Y)
      WRITE(6,300) NUMBER,ITIME,FLAT,FLONG,GRIDI,GRIDJ
  300 FORMAT('0',2I7,5X,'LAT=',F5.1,5X,'LONG=',F7.1 ,5X,'I=',F5.2,5X,
     1  'J=',F5.2,5X)
C
      DO 41 M=1,2
      DO 44 J=1,63
      DO 44 I=1,63
      F(I,J)=HT12HR(I,J,M)
   44 CONTINUE
C
      I=GRIDI
      FI=I
      S=GRIDI - FI
      J=GRIDJ
```

```
      FJ=J
      R=GRIDJ - FJ
C
C
C     ROW INTERPOLATION
      I=I-1
      DO 140 K=1,4
      F1(K)=(F(I,J+1) + F(I,J))/2.0
      F2(K)=F(I,J+1) - F(I,J)
      F3(K)=(F(I,J+2) - F(I,J+1) + F(I,J-1) - F(I,J))/2.0
      FS(K)=F1(K) + (S-.5)*F2(K) + 0.5*S*(S-1.0)*F3(K)
      I=I+1
  140 CONTINUE
C
C
C
C     COLUMN INTERPOLATION
      F4=(FS(3) + FS(2))/2.0
      F5=FS(3) - FS(2)
      F6=(FS(4) - FS(3) + FS(1) - FS(2))/2.0
      FP(N) =F4 + (R-0.5)*F5 + 0.5*R*(R-1.0)*F6
C     XX=THE COMPUTED(INTERPOLATED IN SPACE) HT FOR HT12HR FIELD
      XX=FP(N)
      WRITE(6,9) NUMBER,ITIME,GRIDI,GRIDJ,XX
    9 FORMAT('0','SOUNDING',I4,5X,'TIME',I5,/,' ','I=',F6.2,8X,'J=',
     1  F6.2,8X,'INTERPOLATED HT FROM HT12HR FIELD',F8.1)
      IF(ITIME.GT.1200) GO TO 399
      DO 45 J=1,63
      DO 45 I=1,63
      F(I,J)=HT00HR(I,J,M)
   45 CONTINUE
      I=GRIDI
      FI=I
      S=GRIDI - FI
      J=GRIDJ
      FJ=J
      R=GRIDJ - FJ
C
C
C     ROW INTERPOLATION
      I=I-1
      DO 150 K=1,4
      F1(K)=(F(I,J+1) + F(I,J))/2.0
      F2(K)=F(I,J+1) - F(I,J)
      F3(K)=(F(I,J+2) - F(I,J+1) + F(I,J-1) - F(I,J))/2.0
      FS(K)=F1(K) + (S-.5)*F2(K) + 0.5*S*(S-1.0)*F3(K)
      I=I+1
  150 CONTINUE
```

```
C
C
C
C     COLUMN INTERPOLATION
      F4=(FS(3) + FS(2))/2.0
      F5=FS(3) - FS(2)
      F6=(FS(4) - FS(3) + FS(1) - FS(2))/2.0
      FP(N) =F4 + (R-0.5)*F5 + 0.5*R*(R-1.0)*F6
C     YY=THE COMPUTED(INTERPOLATED IN SPACE) HT FOR HTOOHR FIELD
      YY=FP(N)
      WRITE(6,3) NUMBER,ITIME,GRIDI,GRIDJ,YY
    3 FORMAT('0','SOUNDING',I4,5X,'TIME',I5,/,' ','I=',F6.2,8X,'J=',
     1  F6.2,8X,'INTERPOLATED HT FROM HTOOHR FIELD',F8.1)
      FMINUT=KTIME1*60. + KTIME2
      PART=FMINUT/720.
      FNWC(M)=YY + PART*(XX-YY)
      GO TO 499
C
C
C
C
C
C     WE GET TO HERE ONLY IF ITIME IS GREATER THAN 1200.
  399 DO 46 J=1,63
      DO 46 I=1,63
      F(I,J)=HT24HR(I,J,M)
   46 CONTINUE
C
C
C
C
      I=GRIDI
      FI=I
      S=GRIDI - FI
      J=GRIDJ
      FJ=J
      R=GRIDJ - FJ
C
C
C     ROW INTERPOLATION
      I=I-1
      DO 170 K=1,4
      F1(K)=(F(I,J+1) + F(I,J))/2.0
      F2(K)=F(I,J+1) - F(I,J)
      F3(K)=(F(I,J+2) - F(I,J+1) + F(I,J-1) - F(I,J))/2.0
      FS(K)=F1(K) + (S-.5)*F2(K) + 0.5*S*(S-1.0)*F3(K)
      I=I+1
  170 CONTINUE
```

```
C
C
C
C     COLUMN INTERPOLATION
      F4=(FS(3) + FS(2))/2.0
      F5=FS(3) - FS(2)
      F6=(FS(4) - FS(3) + FS(1) - FS(2))/2.0
      FP(N) =F4 + (R-0.5)*F5 + 0.5*R*(R-1.0)*F6
C     ZZ=THE COMPUTED(INTERPOLATED IN SPACE) HT FOR HT24HR FIELD
      ZZ=FP(N)
      WRITE(6,4) NUMBER,ITIME,GRIDI,GRIDJ,ZZ
    4 FORMAT('0','SOUNDING',I4,5X,'TIME',I5,/,' ','I=',F6.2,8X,'J=',
     1  F6.2,8X,'INTERPOLATED HT FROM HT24HR FIELD',F8.1)
      FMINUT=KTIME1*60. + KTIME2
      PART=(FMINUT-720.)/720.
      FNWC(M)=XX + PART*(ZZ-XX)
  499 WRITE(6,599) NUMBER,ITIME,FLAT,FLONG,FNWC(M)
  599 FORMAT('0','SOUNDING #',I3,5X,'TIME=',I5,5X,'LAT/LONG=',2F8.1,
     1 '    INTERPOLATED HT=',F8.1,/////)
   41 CONTINUE
      WRITE(7,540) IMO,IDA,ITIME,FNWC(1),FNWC(2),NUMBER
  540 FORMAT(I2,1X,I2,1X,I4,'    FNWC HTS',2F10.1,T78,I3)
      NUMBER=NUMBER+1
   88 CONTINUE
      STOP
      END
```

LIST OF REFERENCES

1. Dixon, W. J., Biomedical Computer Programs, Los Angeles, Health Sciences Computing Facility, University of California, Los Angeles, 585 pp., 1966.

2. Elsberry, R. L., and Martin, F. L., "An Experimental Method of Determining Ballistic Densities Making Direct Use of SIRS Radiances," Rept. No. NPS-51ES, MR71101A, Naval Postgraduate School, Monterey, 18 pp., 1971.

3. NIMBUS III User's Guide, Goddard Space Flight Center, Greenbelt, Md., 238 pp., 1969.

4. NIMBUS IV User's Guide, Goddard Space Flight Center, Greenbelt, Md., 214 pp., 1970.

5. Smith, W. L., "Iterative Solution of the Radiative Transfer Equation for the Temperature and Absorbing Gas Profile of an Atmosphere," Applied Optics, Vol. 9, pp. 1993-1999, September 1970.

6. Smith, W. L., Woolf, H. M., and Jacob, W. J., "A Regression Method for Obtaining Real-Time Temperature and Geopotential Height Profiles from Satellite Spectrometer Measurements and its Application to NIMBUS III "SIRS" Observations," Monthly Weather Review, Vol. 98, pp. 582-603, August 1970.

INITIAL DISTRIBUTION LIST

		No. Copies
1.	Lieutenant Robert A. Stanfield CARRIER DIVISION SEVEN FPO, San Francisco, California 96601	5
2.	Professor F. L. Martin Department of Meteorology, Code 51 Mr Naval Postgraduate School Monterey, California 93940	3
3.	Department of Meteorology Naval Postgraduate School Monterey, California 93940	3
4.	Library, Code 0212 Naval Postgraduate School Monterey, California 93940	2
5.	Defense Documentation Center Cameron Station Alexandria, Virginia 22314	2
6.	Professor R. L. Elsberry Department of Meteorology, Code 51 Es Naval Postgraduate School Monterey, California 93940	1
7.	Officer-in-Charge Project FAMOS 3737 Branch Avenue, Room 307 Hillcrest Heights, Maryland 20031	1
8.	Commanding Officer Fleet Numerical Weather Central Monterey, California 93940	1
9.	Naval Weather Service Command Washington Navy Yard Washington, D. C. 20390	1

Unclassified
Security Classification

DOCUMENT CONTROL DATA - R & D

(Security classification of title, body of abstract and indexing annotation must be entered when the overall report is classified)

1. ORIGINATING ACTIVITY *(Corporate author)* Naval Postgraduate School Monterey, California 93940	2a. REPORT SECURITY CLASSIFICATION Unclassified 2b. GROUP

3. REPORT TITLE

Regression Relationships Between Satellite Infrared Radiances and Geopotential Heights of the 500 mb and 300 mb Levels

4. DESCRIPTIVE NOTES *(Type of report and inclusive dates)*
Master's Thesis; March 1972

5. AUTHOR(S) *(First name, middle initial, last name)*

Robert A. Stanfield

6. REPORT DATE March 1972	7a. TOTAL NO. OF PAGES 60	7b. NO. OF REFS 6

8a. CONTRACT OR GRANT NO. b. PROJECT NO. c. d.	9a. ORIGINATOR'S REPORT NUMBER(S) 9b. OTHER REPORT NO(S) *(Any other numbers that may be assigned this report)*

10. DISTRIBUTION STATEMENT

Approved for public release; distribution unlimited.

11. SUPPLEMENTARY NOTES	12. SPONSORING MILITARY ACTIVITY

13. ABSTRACT

Least squares methods are used with NIMBUS IV SIRS-B clear-column radiances as independent variables and two identical-period sources of geopotential heights (at the 500 mb and 300 mb pressure levels) as dependent variables. Regression equations are developed for each of the sets of geopotential heights for three latitude bands in the Northern Hemisphere. Three-day and four-day data bases were used on each regression specification. Each set of equations was tested on independent data at a subsequent composite period of 12-hours and 24-hours following the dependent pooled samples. The regression results of both the dependent and independent tests were examined for possible operational usefulness.

Unclassified
Security Classification

14 KEY WORDS	LINK A		LINK B		LINK C	
	ROLE	WT	ROLE	WT	ROLE	WT
Regression equations						
Geopotential heights						
Satellite radiances						

DD FORM 1 NOV 65 1473 (BACK)
S/N 0101-807-6821

Unclassified
Security Classification

A-31409

Thesis 134155
S6732 Stanfield
c.1 Regression relationships between satellite infrared radiances and geopotential heights of the 500 mb and 300 mb levels.